Hybrid reflections from multiple x-ray scattering in epitaxial oxide films

Eva H. Smith, Phil D. C. King, Arsen Soukiassian, Dieter G. Ast, and Darrell G. Schlom

Citation: Appl. Phys. Lett. **111**, 131903 (2017); doi: 10.1063/1.4993477
View online: http://dx.doi.org/10.1063/1.4993477
View Table of Contents: http://aip.scitation.org/toc/apl/111/13
Published by the American Institute of Physics

Hybrid reflections from multiple x-ray scattering in epitaxial oxide films

Eva H. Smith,[1] Phil D. C. King,[2,3,a)] Arsen Soukiassian,[1] Dieter G. Ast,[1] and Darrell G. Schlom[1,3,b)]
[1]Department of Materials Science and Engineering, Cornell University, Ithaca, New York 14853, USA
[2]Department of Physics, Cornell University, Ithaca, New York 14853, USA
[3]Kavli Institute at Cornell for Nanoscale Science, Ithaca, New York 14853, USA

(Received 28 June 2017; accepted 30 August 2017; published online 29 September 2017)

In numerous symmetric θ-2θ scans of phase-pure epitaxial complex oxide thin films grown on single-crystal substrates, we observe x-ray diffraction peaks that correspond to neither the film nor the substrate crystal structure. These peaks are the result of multiple, sequential diffraction events that occur from both the film and the substrate. The occurrence of so-called "hybrid" reflections, while described in the literature, is not widely reported within the complex oxide thin-film community. We describe a simple method to predict and identify peaks resulting from hybrid reflections and show examples from epitaxial complex oxide films belonging to three distinct structural types. *Published by AIP Publishing.* [http://dx.doi.org/10.1063/1.4993477]

Four-circle x-ray diffraction (XRD) is an essential tool for the characterization of epitaxial thin films, giving information about crystalline phases present, their orientation, and structural perfection. Of particular importance is the ability of x-ray diffraction to determine whether a particular sample consists of a single crystalline phase or a mixture of crystalline phases. For a phase identification to be considered correct, all features (peaks in intensity) in a scan of intensity vs. 2θ must be identified. Any unidentified peaks call into question the phase purity of the thin film.

Multiple scattering events have been described in x-ray diffraction since 1937 as causing unexpected intensity at symmetry-forbidden reflections from single crystals.[1] More recently, hybrid scattering events, in which a beam that is diffracted by the substrate is then diffracted a second time by the film (or vice-versa),[2] have been identified as giving rise to reflections that correspond to neither the film reciprocal lattice nor the substrate reciprocal lattice, but rather a "hybrid" reciprocal lattice, whose reflections are measured at angles 2θ at which neither film nor substrate reflections occur.[3]

Almost every discussion or report in the literature of hybrid reflections in x-ray diffraction experiments uses either synchrotron radiation sources or reciprocal-space maps to search for hybrid reflections and to characterize them.[3–11] These methods, while giving a great deal of information, require either specialized facilities or a significant time investment to perform; the reports themselves employ a deliberate search for hybrid reflections, whereas we now wish to unambiguously identify hybrid reflections in diffraction experiments designed to collect other kinds of information. Discussion of hybrid reflections from complex oxide thin films is at present quite limited in scope.[12,13] We argue here that such reflections may in fact be sufficiently common even in θ-2θ scans measured on commercial diffractometers that checking for hybrid reflections should be a matter of course whenever analyzing diffraction data from high-quality complex oxide thin films.

We may calculate the angle 2θ at which a hybrid reflection is expected to occur in the following way. Consider the hybrid reflection arising from the $h_s k_s \ell_s$ reflection from a substrate with reciprocal lattice vectors $\vec{a}_s^*$, $\vec{b}_s^*$, $\vec{c}_s^*$ and the $h_f k_f \ell_f$ reflection from a film with reciprocal lattice vectors $\vec{a}_f^*$, $\vec{b}_f^*$, $\vec{c}_f^*$. We define reciprocal lattice vectors from the real-space lattice vectors $\vec{a}$, $\vec{b}$, $\vec{c}$ as follows:

$$\vec{a}^* = \frac{\vec{b}\times\vec{c}}{\vec{a}\cdot\vec{b}\times\vec{c}}; \quad \vec{b}^* = \frac{\vec{c}\times\vec{a}}{\vec{a}\cdot\vec{b}\times\vec{c}}; \quad \vec{c}^* = \frac{\vec{a}\times\vec{b}}{\vec{a}\cdot\vec{b}\times\vec{c}}. \tag{1}$$

The scattering vector of the hybrid reflection $\vec{G}_u$ will be the sum of the scattering vectors[3,14,15] of the reflection from the substrate, $\vec{G}_s$, and the reflection from the film, $\vec{G}_f$:

$$\begin{aligned} \vec{G}_s &= h_s\vec{a}_s^* + k_s\vec{b}_s^* + \ell_s\vec{c}_s^* \\ \vec{G}_f &= h_f\vec{a}_f^* + k_f\vec{b}_f^* + \ell_f\vec{c}_f^* \\ \vec{G}_u &= \vec{G}_f + \vec{G}_s. \end{aligned} \tag{2}$$

Bragg's law may be used to find the angle 2θ at which the peak occurs

$$2\theta = 2\arcsin\left(\frac{\lambda|\vec{G}_u|}{2}\right). \tag{3}$$

For coherently strained, epitaxial films grown cube-on-cube relative to their substrates, the in-plane lattice vectors of the film and substrate are the same, i.e., $\vec{a}_s^* = \vec{a}_f^*$ and $\vec{b}_s^* = \vec{b}_f^*$. Then, when $h_s = -h_f$ and $k_s = -k_f$, the in-plane component of the hybrid reflection $h_s\vec{a}_s^* + h_f\vec{a}_f^* + k_s\vec{b}_s^* + k_f\vec{b}_f^*$ is null, and the resulting hybrid reflection is a symmetric reflection, which can be observed during ordinary θ-2θ x-ray diffraction scans.[3]

Many epitaxial oxide thin films grown by pulsed-laser deposition (PLD), molecular-beam epitaxy (MBE), and chemical vapor deposition (CVD) are grown with high structural

a)Current address: School of Physics and Astronomy, University of St. Andrews, St. Andrews, Fife KY16 9SS, United Kingdom.
b)Author to whom correspondence should be addressed: schlom@cornell.edu

quality.[16–26] (We describe specific structural quality criteria below.) For such high-quality films, we present a simple relationship between film and substrate lattice constants and the angles 2θ at which hybrid reflections can be expected to occur. For substrates and films with cubic, tetragonal, or orthorhombic symmetry, the norm of the hybrid scattering vector $|\vec{G}_u|$ relates to the scalar substrate out-of-plane lattice parameter, c_s, and the scalar film out-of-plane lattice parameter, c_f, by

$$|\vec{G}_u| = \left| \frac{\ell_s}{c_s} + \frac{\ell_f}{c_f} \right|, \tag{4}$$

and the angle 2θ at which this reflection is observed is found by substituting the value of $|\vec{G}_u|$ from Eq. (4) into Eq. (3):

$$2\theta = 2\arcsin\left(\frac{\lambda}{2} \left| \frac{\ell_s}{c_s} + \frac{\ell_f}{c_f} \right| \right). \tag{5}$$

For the hybrid reflection to be detected in reflection rather than transmission geometry, as is the case for standard θ-2θ XRD scans, it must be true that both $\ell_s \geq 0$ and $\ell_s/c_s + \ell_f/c_f \geq 0$. ℓ_s and ℓ_f are, of course, integers. We use Eq. (5) with these preceding restrictions to predict the angles in 2θ at which hybrid reflections may be expected to occur.

In addition to comparing predicted 2θ values for hybrid reflections to peak positions measured experimentally, we also identify hybrid reflections through the dependence of their intensity on azimuthal rotation angle ϕ. In contrast to symmetric reflections from the film or substrate, the intensity of hybrid reflections is strongly dependent on ϕ, showing up to hundreds of distinct peaks as intensity is measured as a function of the azimuthal angle.[1,14,15,27] This dependence may be understood by the fact that while these hybrid reflections have no net in-plane scattering component, they arise as a sum of reflections that do, in general, have finite in-plane components. Measuring the ϕ-dependence of a peak present in a θ-2θ scan is a traditional method for identifying the contribution of multiple diffraction events to its intensity.[1,5,14,15]

In the examples that follow, we focus our discussion on the appearance of hybrid reflections in θ-2θ scans, a standard XRD scan for phase characterization,[28] and their verification with ϕ scans. We identify hybrid reflections by ℓ_s and ℓ_f, rather than the sum $\ell_s + \ell_f$, due to the fact that the sum does not uniquely identify a particular reflection (e.g., as seen in Fig. 1(a), the 2_s-1_f hybrid will be measured at a different angle than the 3_s-2_f hybrid; in both cases, $\ell_s + \ell_f = 1$). We do not specify the in-plane components h, k because that information is not readily apparent in the θ-2θ scan. Due to the increasing numbers of reports of high-quality, heteroepitaxial oxide films, we expect that hybrid reflections are observed more commonly than they are mentioned in the literature.

We consider the x-ray diffraction patterns from three films: 50 nm-thick $PbTiO_3/SrTiO_3$ (001); 25 nm-thick La_2NiO_4/LSAT (001), where LSAT refers to $(LaAlO_3)_{0.29}(SrAl_{1/2}Ta_{1/2}O_3)_{0.71}$; and a 190 nm-thick superlattice $[(BaTiO_3)_8/(SrTiO_3)_4]_{40}/TbScO_3$ (110). $PbTiO_3$ is a tetragonal perovskite at room temperature with space group $P4mm$. La_2NiO_4 is the $n = 1$ member of the homologous

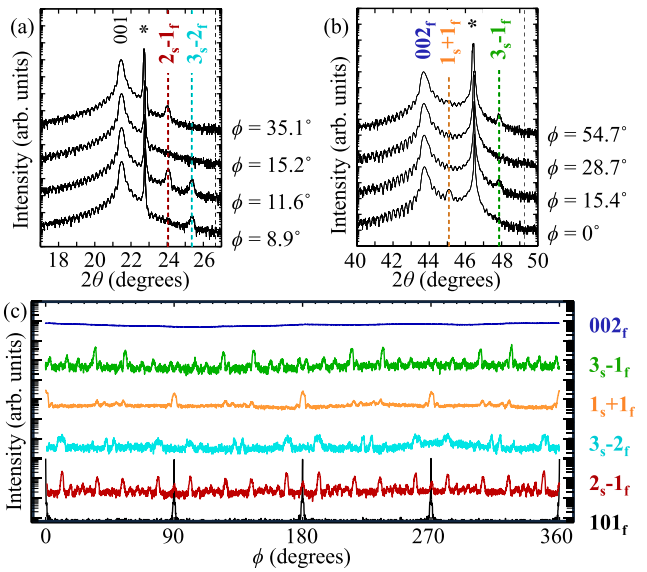

FIG. 1. Dependence of regular and hybrid reflections on (a) and (b) 2θ and (c) ϕ in a 50 nm-thick film of $PbTiO_3$ grown on $SrTiO_3$ (001). The dashed lines in the θ-2θ scan correspond to the expected positions of hybrid reflections calculated using Eq. (5).

Ruddlesden-Popper series[29–31] $La_{n+1}Ni_nO_{3n+1}$ and occurs in the orthorhombic space group $Bmab$ at room temperature.[32] The $[(BaTiO_3)_8/(SrTiO_3)_4]_{40}$ superlattice unit cell, consisting of twelve perovskite pseudocubic units, may have space group[33] $P4mm$ or Cm. For each film, we present θ-2θ patterns taken at several values of ϕ and observe how the peaks arising from hybrid reflections change dramatically in intensity as a function of ϕ while the peaks arising from single diffraction from the film or substrate stay constant. We also present ϕ scans of the hybrid reflections.

The thin films were grown by reactive molecular-beam epitaxy on three different single-crystal substrates. $SrTiO_3$ is a cubic perovskite at room temperature with space group $Pm\bar{3}m$. $TbScO_3$ is an orthorhombic perovskite at room temperature[34] with space group $Pbnm$. LSAT is a tetragonal perovskite[35,36] at room temperature with space group $I\bar{4}$, but its $c/(\sqrt{2}a)$ ratio, 0.999, is so close to unity that we refer to it by its pseudocubic indices.

$PbTiO_3$ was grown in an adsorption-controlled growth regime using a procedure described elsewhere.[37] In short, the substrate temperature was 580 °C, the lead flux was 2×10^{14} atoms $cm^{-2}s^{-1}$, the titanium flux was 9×10^{12} atoms $cm^{-2}s^{-1}$, the distilled ozone ($\sim$80% O_3 + 20% O_2) background pressure was 6×10^{-6} Torr, and all constituent molecular beams were supplied at the same time (continuous codeposition). The $SrTiO_3$ (001) substrate on which the $PbTiO_3$ was grown was TiO_2-terminated.[38] La_2NiO_4 was grown on (001) LSAT, as described previously.[39] In short, the film was grown by sequential deposition of binary oxide monolayers $[LaO\text{-}NiO_2\text{-}LaO]_{40}$ in an atmosphere of 1×10^{-5} Torr distilled ozone and at a substrate temperature of 550 °C. The $[(BaTiO_3)_8/(SrTiO_3)_4]_{40}$ superlattice was grown on $TbScO_3$ (110) as described previously.[40] In short, the film was grown by sequential deposition of binary oxide monolayers BaO, SrO, and TiO_2 following the order in the desired superlattice in an atmosphere of 5×10^{-7} Torr molecular oxygen and at a substrate temperature of 650 °C.

XRD measurements were performed at room temperature on a Rigaku SmartLab using Cu $K\alpha_1$ radiation[41] ($\lambda = 1.5406$ Å) monochromated with a double crystal Ge 220 monochromator. Film out-of-plane lattice parameters are found using Nelson-Riley fitting[42] of the 00ℓ film peak positions from symmetric θ-2θ scans. In the ϕ scans, $\phi = 0$ corresponds to where the in-plane component of the diffraction vector is aligned parallel to the $[100]^*$ direction of the substrate for films grown on cubic substrates or the $[110]^*$ direction (pseudocubic $[100]^*$ direction) of the substrate for the film grown on an orthorhombic $TbScO_3$ substrate. ϕ scans verifying that all three films are grown epitaxially on their substrates are given in the supplementary material.

In Fig. 1, we show θ-2θ scans [(a) and (b)] and ϕ scans (c) of a 50 nm-thick $PbTiO_3/SrTiO_3$ (001) sample. As ϕ is changed, four extra peaks beyond what would be expected from a superposition of the $SrTiO_3$ and $PbTiO_3$ patterns appear and disappear in the θ-2θ scan: two extra peaks near the film and substrate 001 reflections and two extra peaks near the film and substrate 002 reflections. Using the measured c-lattice constant for this $PbTiO_3$ film of 4.138 Å and a c-lattice constant of 3.905 Å for the $SrTiO_3$ substrate,[43] Eq. (5) predicts that hybrid reflections between $PbTiO_3$ and $SrTiO_3$ will occur at the angles marked with dashed lines in the θ-2θ scans of Figs. 1(a) and 1(b). All four extra peaks fall at angles predicted for hybrid reflections.

To solidify our belief that the "extra" peaks result from hybrid reflections, we rotate the sample about ϕ and measure the changing x-ray intensity at each of the four extra reflections. For reference, we also measure how the intensity of a symmetric, singly diffracted film reflection varies with ϕ. We also measure the intensity of the film 101 peak, an asymmetric reflection, as a function of ϕ to provide a reference angle for the ϕ scans. The symmetric film and hybrid reflections depend very differently on ϕ. The intensity of the $PbTiO_3$ 002 reflection is nearly constant as a function of ϕ, while the intensities of the hybrid reflections vary rapidly.

We next consider hybrid reflections from a Ruddlesden-Popper film, a structural relative to the perovskite. θ-2θ scans at various ϕ, and ϕ-scans at various values of 2θ, from a 25-nm-thick film of La_2NiO_4 grown on LSAT (001) are shown in Fig. 2. Four hybrid reflections appear in the θ-2θ XRD patterns near the film 002 and the film 006 reflections, shown in Figs. 2(a) and 2(b), respectively. The hybrid reflections appear at the values of 2θ predicted using Eq. (5) with the pseudocubic lattice constant[35,36] of LSAT, c_s=3.866 Å and the measured out-of-plane lattice constant of the film, c_f = 12.670 Å. The many discrete peaks of intensity in ϕ seen in Fig. 2(c) further support our belief that these four extra reflections are also due to hybrid diffraction.

Last, we consider hybrid reflections from a superlattice film, a film whose unit cell is a stack of eight $BaTiO_3$ pseudocubic units and four $SrTiO_3$ pseudocubic units, repeated 40 times ($[(BaTiO_3)_8/(SrTiO_3)_4]_{40}$), grown on a $TbScO_3$ substrate. The surface lattice of the $TbScO_3$ (110) face is not a perfect square due to the fact that $TbScO_3$ is orthorhombic (the in-plane pseudocubic lattice constants[34] differ by 0.001 Å); in spite of this slight mismatch between the film and substrate symmetries, we observe three hybrid reflections from this sample, at angles calculated using Eq. (5)

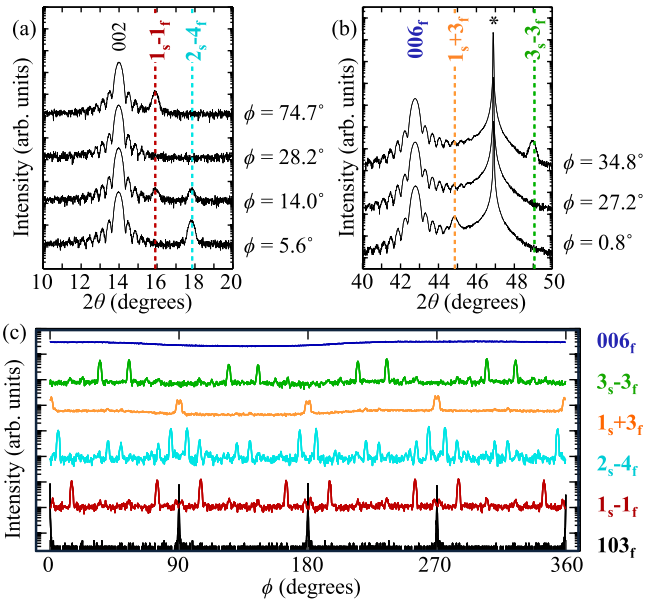

FIG. 2. Dependence of regular and hybrid reflections on (a) and (b) 2θ and (c) ϕ in a 25-nm-thick film of La_2NiO_4 grown on LSAT (001). The dashed lines in (a) and (b) correspond to the expected positions of hybrid reflections calculated using Eq. (5).

with our measured film out-of-plane lattice constant of 48.24 Å and a pseudocubic substrate lattice constant[34] of 3.950 Å. Figure 3(a) shows two hybrid reflections appearing and disappearing near in 2θ to the film $00\underline{12}$ reflection. Another hybrid reflection appears in 2θ just off the film $00\underline{25}$ reflection, shown in Fig. 3(b). The first two hybrid reflections show the same dependence on ϕ, as seen in Fig. 3(c), while the third hybrid reflection shows independent behavior in ϕ.

Based on the appearance of hybrid reflections in the three films belonging to three distinct structural types, we believe that it is likely that such hybrid reflections may occur in symmetric θ-2θ scans of high-crystalline quality thin films

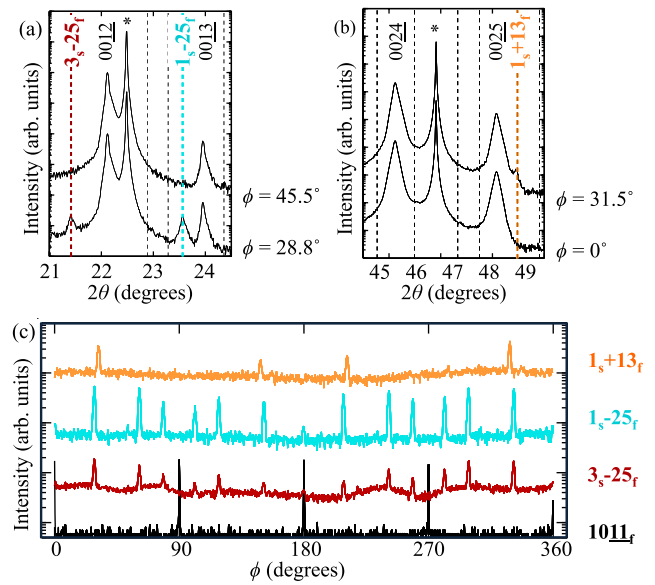

FIG. 3. Dependence of regular and hybrid reflections on (a) and (b) 2θ and (c) ϕ in a 190-nm-thick film of a $[(BaTiO_3)_8(SrTiO_3)_4]_{40}$ superlattice grown on $TbScO_3$ (110). The dashed lines in (a) and (b) correspond to the expected positions of hybrid reflections calculated using Eq. (5).

as long as those films meet the crystallographic requirements described below. Such peaks will furthermore be detectable with a commercial benchtop diffractometer when the intensity of an x-ray beam diffracted (once) from the film is sufficiently large. This latter condition is met if the film is sufficiently thick, the film contains a high concentration of atoms with a high atomic number, the film and substrate have a sufficiently large number of high-intensity reflections, or the x-ray source is sufficiently bright. We may estimate an upper bound for the intensity of a hybrid reflection using a procedure described in the supplementary material. Based on this method, we calculate that the most intense hybrid reflections from the $PbTiO_3/SrTiO_3$ (001) film and from the La_2NiO_4/LSAT (001) film each combine the most intense substrate-only reflection with the most intense film-only reflection; this prediction is in agreement with our observations for these samples.

In deriving Eq. (5), we assumed that the film would be coherently strained, epitaxial, and grown cube-on-cube relative to the substrate. Growth of single-crystal, coherently strained, heteroepitaxial oxide films with high structural perfection (film rocking curve full width at half maximum $\leq 0.01^\circ$) is increasingly common[16–18] and also increasingly accessible.[44]

Interestingly, we also observed hybrid reflections from films that do not strictly meet all these structural criteria. We show in Fig. 3 hybrid reflections from a tetragonal (or monoclinic) film grown on an orthorhombic substrate. While this film is not strictly cube-on-cube relative to its substrate, we could approximate the epitaxial relationship between the film and the substrate as "cube-on-pseudocube" (see the comparison of ϕ scans of film and substrate reflections in the supplementary material). We also have observed hybrid reflections from a 300-nm thick film of $PbTiO_3$ grown on $SrTiO_3$ that is relaxed, with a mixture of *a*- and *c*-domains, though still cube-on-cube epitaxial. The hybrid reflections are likely broad in reciprocal space, allowing them to be observed in symmetric θ-2θ scans in spite of the imperfect coherence of the film. Many high-quality, single-crystal, heteroepitaxial oxide films are highly oriented relative to their substrates in-plane, as were these two films, as shown through reciprocal-space maps or reflection high energy electron diffraction of both the film and the substrate.[18–26]

We conclude that hybrid reflections may be expected from heteroepitaxial oxide thin films that: (1) are grown close to cube-on-cube relative to their substrates; (2) have an in-plane lattice constant close to that of the underlying substrate, though which may or may not be perfectly coherent; (3) have low mosaicity;[45] and (4) scatter sufficiently brightly. The combination of more films being grown and studied that meet the criteria for hybrid reflections, with awareness of how to predict and verify hybrid reflections, makes us anticipate that reports of hybrid reflections in the literature will grow. Based on the diversity of films in which we observe such behavior, the fact that we use no special techniques or equipment to collect our diffraction data, and the growing numbers of reports of heteroepitaxial thin films with high crystalline quality, we believe that hybrid reflections may in fact already be more common than they are mentioned in the literature.

See supplementary material for evidence of cube-on-(pseudo)cube epitaxy and an estimate for an upper bound for the intensity of a hybrid reflection.

E.H.S. and D.G.S. acknowledge support by the National Science Foundation (NSF) MRSEC program (DMR-1420620). This work made use of the Cornell Center for Materials Research (CCMR) Shared Facilities, which are supported through the NSF MRSEC program (DMR-1120296). Substrate preparation was performed in part at the Cornell NanoScale Facility, a member of the National Nanotechnology Coordinated Infrastructure (NNCI), which is supported by the National Science Foundation (ECCS-15420819).

[1]M. Renninger, Z. Phys. **106**, 141 (1937).
[2]We do not distinguish between multiple diffraction events occurring in the sequence: substrate, film; from those occurring in the sequence: film, substrate.
[3]S. L. Morelhão and J. Z. Domagała, J. Appl. Crystallogr. **40**, 546 (2007).
[4]B. J. Isherwood, B. R. Brown, and M. A. G. Halliwell, J. Cryst. Growth **54**, 449 (1981).
[5]S. L. Morelhão, L. P. Cardoso, J. M. Sasaki, and M. M. G. de Carvalho, J. Appl. Phys. **70**, 2589 (1991).
[6]S. L. Morelhão and L. P. Cardoso, J. Appl. Phys. **73**, 4218 (1993).
[7]S. L. Morelhão, H. Avanci, M. A. Hayashi, L. P. Cardoso, and S. P. Collins, Appl. Phys. Lett. **73**, 2194 (1998).
[8]S. L. Morelhão, A. A. Quivy, and J. Härtwig, Microelectron. J. **34**, 695 (2003).
[9]A. S. de Menezes, A. O. dos Santos, J. M. A. Almeida, J. R. R. Bortoleto, M. A. Cotta, S. L. Morelhão, and L. P. Cardoso, Cryst. Growth Des. **10**, 3436 (2010).
[10]A. S. de Menezes, G. A. Calligaris, R. Lang, A. O. dos Santos, and L. P. Cardoso, CrystEngComm **15**, 2251 (2013).
[11]J. Z. Domagała, S. L. Morelhão, M. Sarzyński, M. Maździarz, P. Dłużewski, and M. Leszczyński, J. Appl. Crystallogr. **49**, 798 (2016).
[12]A. H. G. Vlooswijk, Ph.D. thesis, University of Groningen, 2009.
[13]S. Saremi, R. Xu, L. R. Dedon, J. A. Mundy, S.-L. Hsu, Z. Chen, A. R. Damodaran, S. P. Chapman, J. T. Evans, and L. W. Martin, Adv. Mater. **28**, 10750 (2016).
[14]H. Cole, F. W. Chambers, and H. M. Dunn, Acta Cryst. **15**, 138 (1962).
[15]S.-L. Chang, *Multiple Diffraction of X-Rays in Crystals*, Springer Series in Solid-State Sciences Vol. 50, edited by M. Cardona, P. Fulde, and H.-J. Queisser (Springer-Verlag, Berlin, 1984) Chap. 2, pp. 7–34.
[16]D. D. Fong, A. M. Kolpak, J. A. Eastman, S. K. Streiffer, P. H. Fuoss, G. B. Stephenson, C. Thompson, D. M. Kim, K. J. Choi, C. B. Eom, I. Grinberg, and A. M. Rappe, Phys. Rev. Lett. **96**, 127601 (2006).
[17]B. Jalan, R. Engel-Herbert, N. J. Wright, and S. Stemmer, J. Vac. Sci. Technol. A **27**, 461 (2009).
[18]J. A. Moyer, C. Eaton, and R. Engel-Herbert, Adv. Mater. **25**, 3578 (2013).
[19]S. J. May, P. J. Ryan, J. L. Robertson, J.-W. Kim, T. S. Santos, E. Karapetrova, J. L. Zarestky, X. Zhai, S. G. E. te Velthuis, J. N. Eckstein, S. D. Bader, and A. Bhattacharya, Nat. Mater. **8**, 892 (2009).
[20]H. Boschker, M. Huijben, A. Vailionis, J. Verbeeck, S. van Aert, M. Luysberg, S. Bals, G. van Tendeloo, E. P. Houwman, G. Koster, D. H. A. Blank, and G. Rijnders, J. Phys. D: Appl. Phys. **44**, 205001 (2011).
[21]Y. Matsubara, K. S. Takahashi, Y. Tokura, and M. Kawasaki, Appl. Phys. Express **7**, 125502 (2014).
[22]K. H. L. Zhang, Y. Du, A. Papadogianni, O. Bierwagen, S. Sallis, L. F. J. Piper, M. E. Bowden, V. Shutthanandan, P. V. Sushko, and S. A. Chambers, Adv. Mater. **27**, 5191 (2015).
[23]C. Eaton, J. A. Moyer, H. M. Alipour, E. D. Grimley, M. Brahlek, J. M. LeBeau, and R. Engel-Herbert, J. Vac. Sci. Technol. A **33**, 061504 (2015).
[24]R. C. Haislmaier, E. D. Grimley, M. D. Biegalski, J. M. LeBeau, S. Trolier-McKinstry, V. Gopalan, and R. Engel-Herbert, Adv. Funct. Mater. **26**, 7271 (2016).
[25]S. Raghavan, T. Schumann, H. Kim, J. Y. Zhang, T. A. Cain, and S. Stemmer, APL Mater. **4**, 016106 (2016).
[26]A. K. Yadav, C. T. Nelson, S. L. Hsu, Z. Hong, J. D. Clarkson, C. M. Schlepütz, A. R. Damodaran, P. Shafer, E. Arenholz, L. R. Dedon, D. Chen, A. Vishwanath, A. M. Minor, L. Q. Chen, J. F. Scott, L. W. Martin, and R. Ramesh, Nature **530**, 198 (2016).
[27]E. Rossmanith, J. Appl. Crystallogr. **33**, 921 (2000).

[28]B. D. Cullity and S. R. Stock, *Elements of X-Ray Diffraction*, *Third Edition* (Prentice Hall, Upper Saddle River, New Jersey, 2001), pp. 275–294.
[29]D. Balz and K. Plieth, Z. Elektrochem. **59**, 545 (1955).
[30]S. N. Ruddlesden and P. Popper, Acta Crystallogr. **10**, 538 (1957).
[31]S. N. Ruddlesden and P. Popper, Acta Crystallogr. **11**, 54 (1958).
[32]J. Rodríguez-Carvajal, M. T. Fernández-Díaz, and J. L. Martínez, J. Phys.: Condens. Matter **3**, 3215 (1991).
[33]V. Želený, O. Caha, A. Soukiassian, D. G. Schlom, and X. X. Xi, Phys. Rev. B **95**, 214110 (2017).
[34]R. Uecker, B. Velickov, D. Klimm, R. Bertram, M. Bernhagen, M. Rabe, M. Albrecht, R. Fornari, and D. G. Schlom, J. Cryst. Growth **310**, 2649 (2008).
[35]M. Steins, J. Doerschel, and P. Reiche, Z. Kristallogr. New Cryst. Struct. **212**, 77 (1997).
[36]J. Xiao, M. Shao, Y. Tian, W. Huang, A. Wang, and S. Yin, J. Cryst. Growth **236**, 671 (2002).
[37]E. H. Smith, J. F. Ihlefeld, C. A. Heikes, H. Paik, Y. Nie, C. Adamo, T. Heeg, Z.-K. Liu, and D. G. Schlom, Phys. Rev. Mater. **1**, 023403 (2017).
[38]G. Koster, B. L. Kropman, G. J. H. M. Rijnders, D. H. A. Blank, and H. Rogalla, Appl. Phys. Lett. **73**, 2920 (1998).
[39]P. D. C. King, H. I. Wei, Y. F. Nie, M. Uchida, C. Adamo, S. Zhu, X. He, I. Božović, D. G. Schlom, and K. M. Shen, Nat. Nanotechnol. **9**, 443 (2014).
[40]A. Soukiassian, W. Tian, V. Vaithyanathan, J. H. Haeni, L. Q. Chen, X. X. Xi, D. G. Schlom, D. A. Tenne, H. P. Sun, X. Q. Pan, K. J. Choi, C. B. Eom, Y. L. Li, Q. X. Jia, C. Constantin, R. M. Feenstra, M. Bernhagen, P. Reiche, and R. Uecker, J. Mater. Res. **23**, 1417 (2008).
[41]G. Höltzer, M. Fritsch, M. Deutsch, J. Härtwig, and E. Förster, Phys. Rev. A **56**, 4554 (1997).
[42]J. B. Nelson and D. P. Riley, Proc. Phys. Soc. London **57**, 160 (1945).
[43]*Landolt-Börnstein: Numerical Data and Functional Relationships in Science and Technology, New Series, Group III*, edited by K. H. Hellwege and A. M. Hellwege (Springer, Berlin, 1981), Vol. 16a, p. 59.
[44]See www.paradim.org for details on a new national user facility dedicated to accelerating the rate of discovery of materials for the next generation of electronics–the Platform for the Accelerated Realization, Analysis, and Discovery of Interface Materials (PARADIM).
[45]S. Caticha-Ellis, Acta Crystallogr. A **25**, 666 (1969).